Supporting Information

Hefetz-Sela et al. 10.1073/pnas.1409700111

SI Methods

Mice. Mdr2$^{-/-}$c-Jun$^{WT/WT}$ served as control mice for Mdr2$^{-/-}$c-Jun$^{AA/AA}$, and Mdr2$^{-/-}$c-Jun$^{f/f}$ served as a control for Mdr2$^{-/-}$c-Jun$^{\Delta hep}$. For hepatocarcinogenesis, Mdr2$^{-/-}$c-Jun$^{WT/WT}$ and Mdr2$^{-/-}$c-Jun$^{AA/AA}$ were killed at 11–12 mo of age and Mdr2$^{-/-}$c-Jun$^{f/f}$ and Mdr2$^{-/-}$c-Jun$^{\Delta hep}$ at 14–15 mo of age. BrdU was injected (Amersham; 100 μL per 10 g of body weight) 3 h before death. Animals were killed by a lethal dose of anesthesia and perfused through the left ventricle with heparinized PBS followed by buffered formalin. See Table S2 for genotyping primers.

Histology and Quantification of Tumors. Immediately after death, livers were removed and fixed in 4% (wt/vol) buffered formalin. For macroscopic quantification, externally visible tumors were counted on the liver surface. Microscopic quantification of tumors and examination of liver H&E sections were performed by expert liver pathologists (O.P. and E.P.). Both macroscopic and histologic analyses were performed in a blinded fashion. Serum alanine transaminase (ALT), alkaline phosphatase (ALP), and aspartate aminotransferase (AST/GOT) levels were determined by using the Reflotron Plus analysis system (Roche).

Immunohistochemistry. Antibodies used were as follows: c-Jun (BD Transduction Laboratories; clone 3/Jun); phospho–c-Jun Ser-63 (Cell Signaling; no. 9261); phospho–c-Jun Ser-73 (D47G9) (Cell Signaling; no. 3270); F4/80 (Serotec; CI:A3-1); Foxp3 (eBioscience; no. 14-5773); BrdU (Thermo Scientific; MS-1058-R7); Cleaved caspase-3 (Cell Signaling; no. 9661); CCL17 (R&D; AF529); p53 (Novocastra CM5); and p21 (Santa Cruz; F-5). All stains were performed on 5-μm formalin-fixed paraffin-embedded sections. After antigen retrieval, endogenous peroxidase was blocked by 3% H_2O_2. Afterward, slides were incubated with primary antibody diluted in Cas-block (Zymed), washed, and incubated with the appropriate secondary HRP-conjugated antibody (Dako: mouse; Vector Labs: rabbit; Histofine: rat and goat). Slides were developed with the HRP substrate diaminobenzidine (Thermo Scientific) and counterstained with hematoxylin. Double immunostaining for Foxp3 and CCL17 was performed with the Polink DS-GRT-Hu/Ms Kit (GBI Laboratories).

For quantification of immunostains, stained slides were counted either manually by counting the number of positive cells per 10 high-power fields or quantified with the Ariol SL-50 automated scanning microscope and image-analysis system (Genetix). Briefly, the frequency of positive cells was assessed with the appropriate module of the Ariol SL-50. For each sample, the percentage of positive cells or the intensity of the staining was determined in 10 (arbitrarily chosen) fields.

Chronic Inflammation Induced by Liposomal LPS. Mice were injected s.c. with LPS (*Escherichia coli* strain 055:B5; L-4524; Sigma) encapsulated in multilamellar liposomal vesicles as described (1).

LPS was administered three times, every 5 d at a dose of 70 μg per animal for the induction of chronic inflammation (2). Spleen was weighed, and the percent of Foxp3$^+$CD4$^+$ Treg cells out of splenocytes and out of PBLs was determined by FACS. For FACS analysis, cells were stained with phycoerythrin (PE)-conjugated anti-Foxp3 antibody and FITC-conjugated anti-CD4–FITC antibody (Miltenyi). Samples were analyzed in a FACSCalibur apparatus by using Cell Quest software (BD PharMingen).

Treg Cell Conversion Assay. CD4$^+$CD25$^-$ T cells were isolated from mouse spleens by negative selection (Miltenyi). Cells were >90% pure, as determined by FACS analysis. A total of 1.5 × 10^6 cells per mL of CD4$^+$CD25$^-$ was stimulated with anti-CD3/CD28 (2 μg/mL) ± TGF-β (5 ng/mL) ± IL-2 (25 U/mL) in complete RPMI medium 1640 for 4 d in 24-well plates (3). Upon harvesting, cells were centrifuged and resuspended in PBS containing 1.5% FCS. Cells were stained with surface antibodies allophycocyanin (APC)-conjugated anti-CD25 and FITC-conjugated anti-CD4. Intracellular staining was performed with PE-conjugated anti-Foxp3 (Miltenyi).

Liver Macrophage Isolation. Kupffer cells were isolated from Mdr2$^{-/-}$ mice livers essentially as described by Kamimura and Tsukamoto (4). Livers were digested enzymatically with Pronase (Roche) and Collagenase (Sigma) by in situ perfusion. Nonparenchymal cells were isolated by centrifugation of the digest at 150 × *g* for 8 min and were laid on top of a four density Larcoll gradient. The gradients were centrifuged at 49,280 × *g* for 30 min at 25 °C by using a SW41Ti rotor (Beckman). A pure population of Kupffer cells was recovered from the interface between 8% and 12% Larcoll, washed, and immediately frozen in liquid nitrogen for further analysis. Purity of the Kupffer cell fraction was determined by H&E staining of cytospins preparations and always was >90%.

Macrophage Polarization in Culture. Peritoneal elicited macrophages (PECs) were obtained from mice injected 4 d previously with 1 mL of 3% (wt/vol) Thioglycollate (Difco). A total of 0.25 × 10^6 macrophages per mice was seeded in 4 mL of RPMI medium 1640 containing 10% FBS, 2 mM glutamine, and 100 U/mL penicillin–streptomycin in 60-mm culture dishes, and after 2 h of incubation, nonadherent cells were washed off (×2) with medium. Monolayers were >95% macrophages, as evidenced by morphology. PECs were then incubated for additional 2 h before starting M1- or M2-inducing protocols [described in Porta et al. (5)]: To induce M1 activation, cells were incubated in medium for 20 h, washed, left in medium for 2 h, and finally stimulated with LPS for 4 h. For inducing M2 polarization, two protocols were used: Cells were incubated in the presence of LPS for 20 h, washed, and maintained in RPMI medium for 2 h and then rechallenged with LPS for 4 h (M2a) or cells were treated with LPS for 20 h, washed, and then maintained in medium for an additional 6 h without LPS rechallenge (M2b). Control cells were cultured in medium for the entire period of the experiment. For gene-expression analysis, total RNA was extracted with TRIzol (Invitrogen). LPS concentration for inducing treatments was 100 ng/mL.

In Vivo Migratory Assay of CFSE-Labeled Treg Cells. Splenic CD4$^+$CD25$^+$ Treg cells were purified by using MACS (Miltenyi) from 3-mo-old Mdr2$^{-/-}$c-Jun$^{WT/WT}$ mice and labeled with CFSE (Promega). A total of 5 × 10^5 CFSE-labeled cells were injected through the tail vein into 9-mo-old Mdr2$^{-/-}$c-Jun$^{WT/WT}$ or Mdr2$^{-/-}$c-Jun$^{AA/AA}$ mice. The livers were harvested 48 h after adoptive transfer and dissociated into single cell suspensions, and the percentage of CFSE-labeled cells was determined by FACS.

qPCR. Total RNA was extracted with TRIzol and was reverse-transcribed by the high-capacity cDNA reverse transcription kit (Applied Biosystems). qPCR reactions were run in triplicates in 384-well plates on the AB7900 Real Time PCR system. Platinum Syber mix was used in all experiments. Results were analyzed by

using the Dataassist software (Version 2.0; Applied Biosystems). Every experiment included two out of three reference genes: PP1A, HPRT, or Actin. For details of the exon-skipping primers, see Table S1.

1. Joseph A, et al. (2002) Liposomal immunostimulatory DNA sequence (ISS-ODN): An efficient parenteral and mucosal adjuvant for influenza and hepatitis B vaccines. *Vaccine* 20(27-28):3342–3354.
2. Vaknin I, et al. (2008) A common pathway mediated through Toll-like receptors leads to T- and natural killer-cell immunosuppression. *Blood* 111(3):1437–1447.
3. Davidson TS, DiPaolo RJ, Andersson J, Shevach EM (2007) Cutting edge: IL-2 is essential for TGF-beta-mediated induction of Foxp3+ T regulatory cells. *J Immunol* 178(7):4022–4026.
4. Kamimura S, Tsukamoto H (1995) Cytokine gene expression by Kupffer cells in experimental alcoholic liver disease. *Hepatology* 22(4 Pt 1):1304–1309.
5. Porta C, et al. (2009) Tolerance and M2 (alternative) macrophage polarization are related processes orchestrated by p50 nuclear factor kappaB. *Proc Natl Acad Sci USA* 106(35):14978–14983.

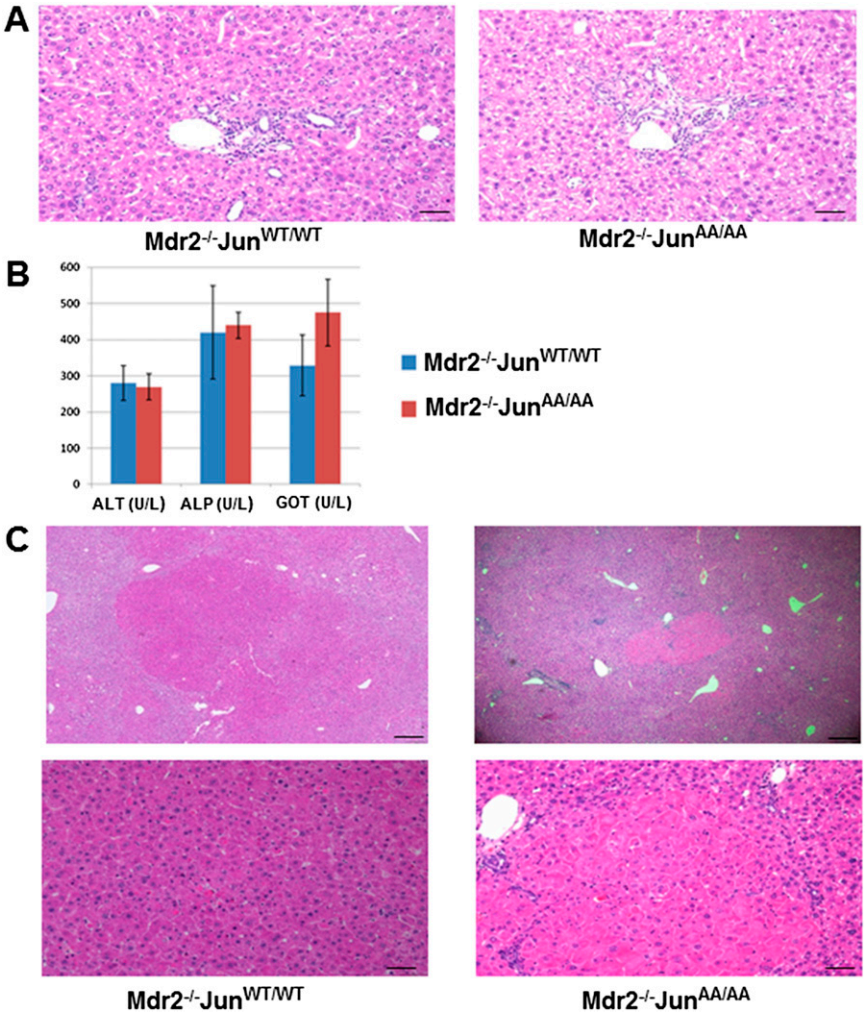

Fig. S1. JNP modulates hepatocarcinogenesis in Mdr2$^{-/-}$ mice. (*A*) Representative H&E-stained sections of liver parenchymas from 7-mo-old mice of the indicated genotypes, showing similar inflammatory infiltrates. (Scale bars: 50 μm.) (*B*) Liver damage markers in sera of 7-mo-old Mdr2$^{-/-}$c-Jun$^{WT/WT}$ and Mdr2$^{-/-}$c-Jun$^{AA/AA}$ mice. Alanine transaminase (ALT), $n = 12$; alkaline phosphatase (ALP) and aspartate aminotransferase/glutamic oxaloacetic transaminase (AST/GOT), $n = 6$. Bars correspond to mean ± SEM. (*C*) Representative H&E-stained sections of liver tumors from 11-mo-old mice of the indicated genotypes, showing reduced tumor diameter in Mdr2$^{-/-}$c-Jun$^{AA/AA}$ mice (*Upper*). *Lower* shows higher magnification of the tumors. (Scale bars: *Upper*, 200 μm; *Lower*, 50 μm.)

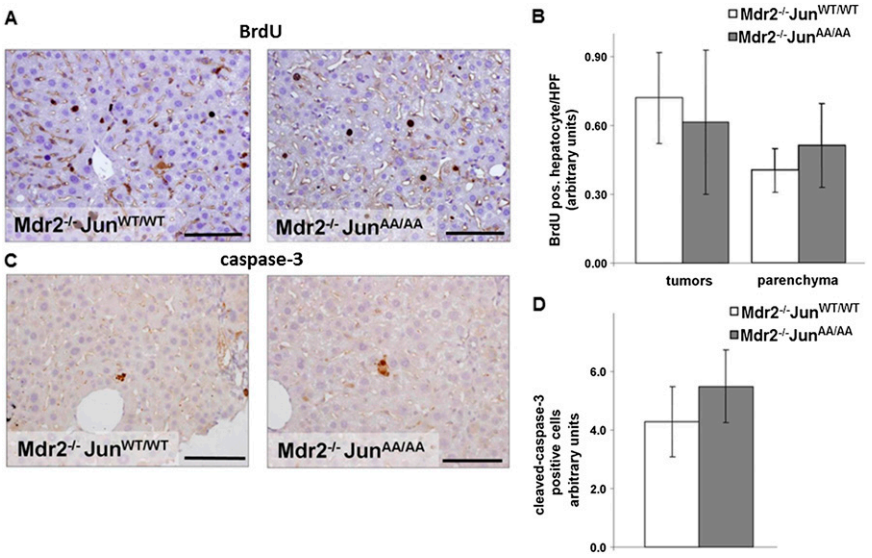

Fig. S2. JNP does not alter proliferation or apoptosis in Mdr2$^{-/-}$ mice. (*A*) Representative photomicrographs of immunostains for the proliferation marker BrdU in liver parenchymas of 11-mo-old Mdr2$^{-/-}$c-Jun$^{WT/WT}$ and Mdr2$^{-/-}$c-Jun$^{AA/AA}$ mice. (Scale bars: 125 μm.) (*B*) Quantification of BrdU-positive hepatocytes in liver parenchyma and tumor tissue (n = 10; bars correspond to mean ± SEM). pos, positive; HPF, high power field. (*C*) Representative photomicrographs of immunostaining for apoptotic cells using anti-cleaved caspase-3 antibody in liver parenchyma of 11-mo-old Mdr2$^{-/-}$c-Jun$^{WT/WT}$ and Mdr2$^{-/-}$c-Jun$^{AA/AA}$ livers. (Scale bars: 125 μm.) (*D*) Quantification of cleaved caspase-3–positive cells in liver parenchyma (n = 7; bars correspond to mean ± SEM).

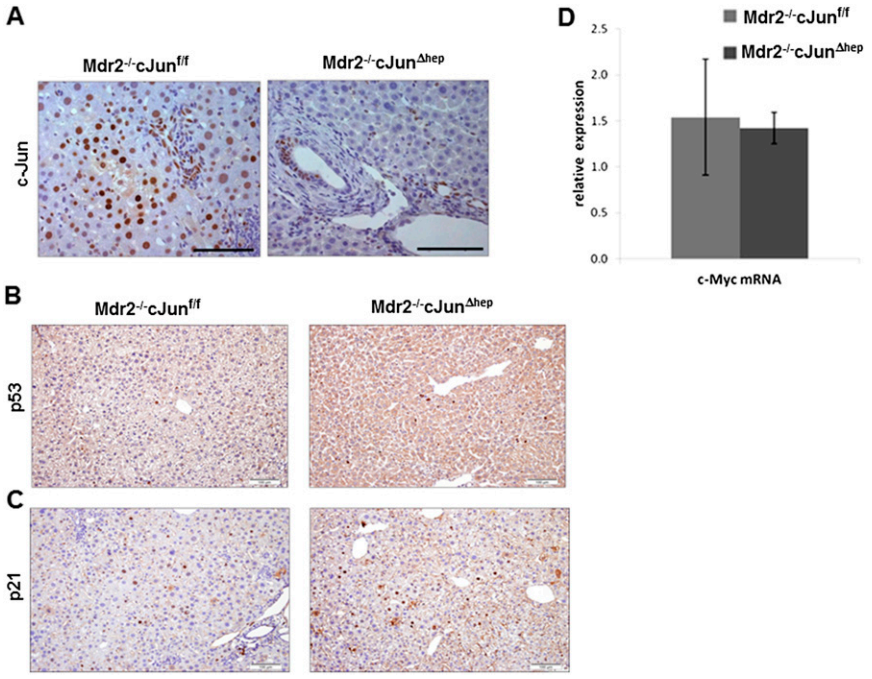

Fig. S3. The p53 axis is not activated in Mdr2$^{-/-}$ liver parenchymas. (*A*) c-Jun immunostains in liver parenchyma of mice with the indicated genotype. (Scale bars: 100 μm.) (*B* and *C*) p53 (*B*) and p21 (*C*) immunostains in liver parenchymas of 15-mo-old Mdr2$^{-/-}$c-Jun$^{f/f}$ and Mdr2$^{-/-}$c-Jun$^{\Delta hep}$ mice. (Scale bars: 100 μm.) (*D*) qPCR analysis of c-Myc mRNA levels in liver lysates of 15-mo-old Mdr2$^{-/-}$c-Jun$^{f/f}$ or Mdr2$^{-/-}$c-Jun$^{\Delta hep}$ mice (n = 6; bars correspond to mean ± SEM).

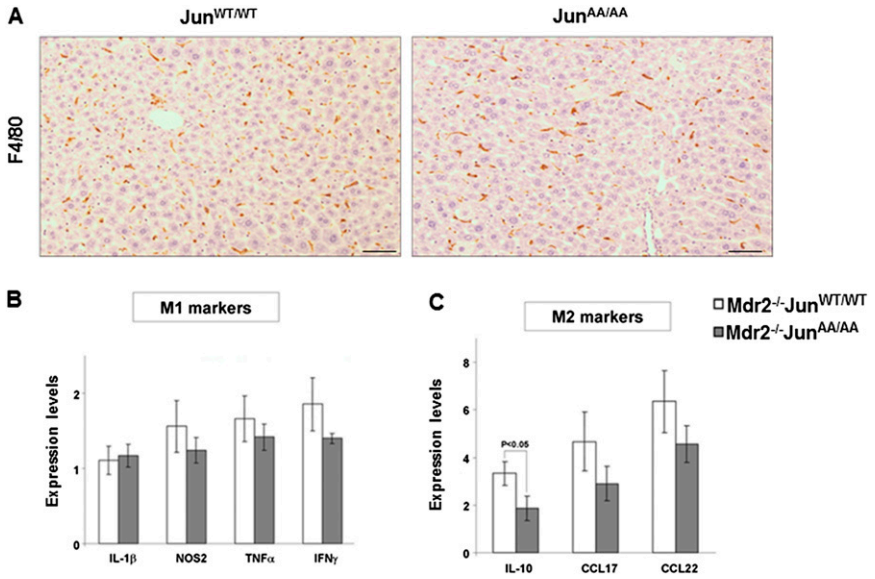

Fig. S4. Kupffer cell numbers are not affected by JNP in the noninflamed liver. (*A*) Representative immunostains for the macrophage marker F4/80 in liver parenchymas of c-Jun$^{WT/WT}$ and c-Jun$^{AA/AA}$ mice, both harboring the WT Mdr2 allele. (Scale bars: 100 μm.) (*B* and *C*) qPCR analysis for M1 (*B*) and M2 (*C*) markers in total liver lysates from 11-mo-old Mdr2$^{-/-}$c-Jun$^{WT/WT}$ or Mdr2$^{-/-}$c-Jun$^{AA/AA}$ mice ($n = 9$; mean ± SEM).

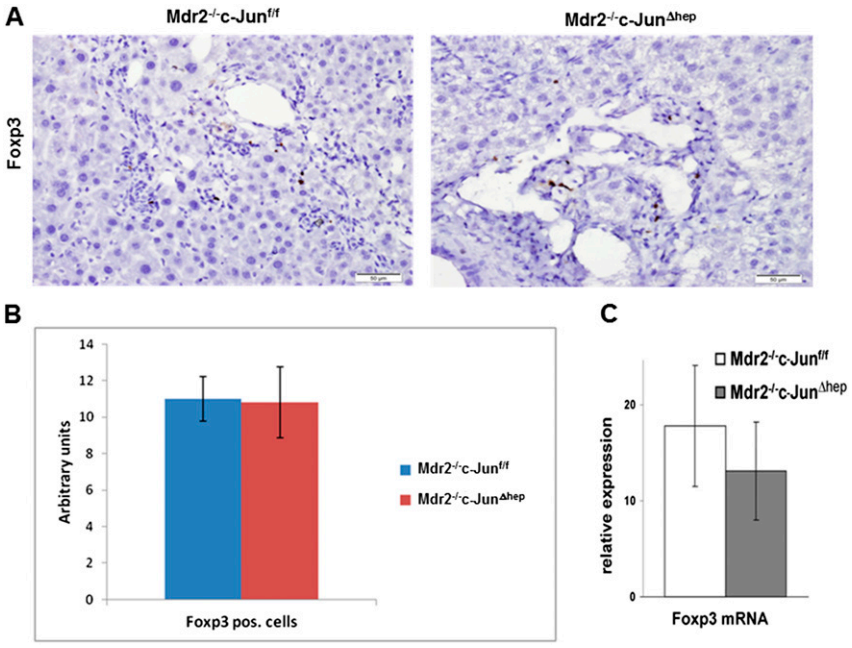

Fig. S5. Deleting hepatocyte c-Jun does not affect Treg cell numbers in Mdr2$^{-/-}$ mice. (*A*) Representative immunostains for Foxp3 in liver parenchymas of 15-mo-old Mdr2$^{-/-}$c-Jun$^{f/f}$ and Mdr2$^{-/-}$c-Jun$^{\Delta hep}$ mice. (Scale bars: 50 μm.) (*B*) Quantification of Foxp3 immunostaining ($n \geq 11$; bars correspond to mean ± SEM). pos, positive. (*C*) qPCR analysis of Foxp3 expression in liver lysates of 15-mo-old mice ($n = 5$; mean ± SEM).

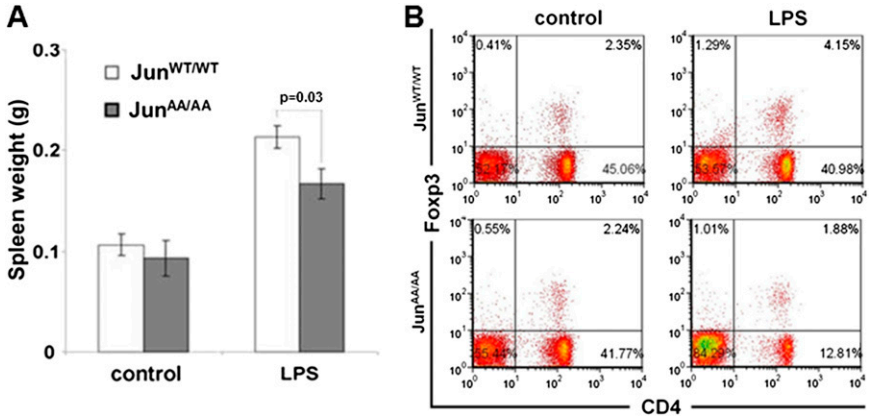

Fig. S6. Treg accumulation depends on JNP. Liposomal LPS induced chronic inflammation. (*A*) Spleen weights (n = 3; mean ± SEM). (*B*) FACS dot plots of Foxp3-positive vs. CD4-positive cells in PBLs.

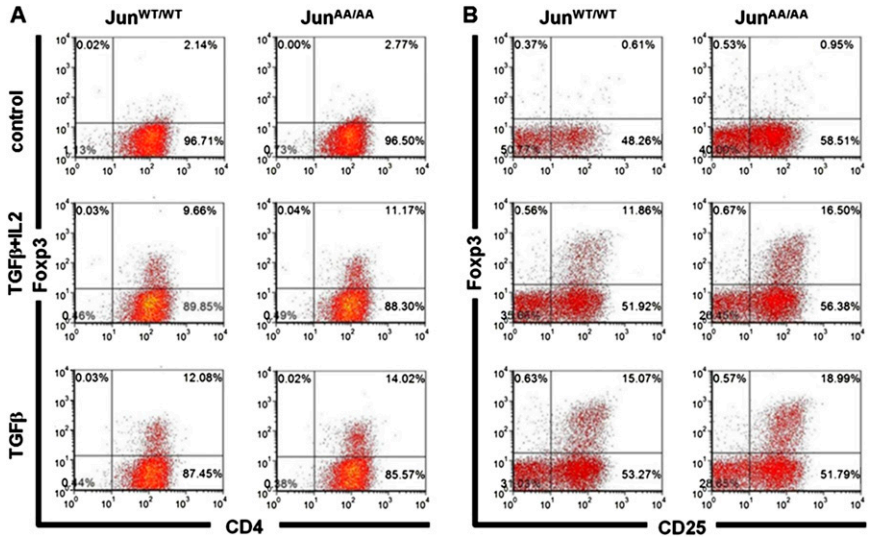

Fig. S7. JNP is not necessary for generation of inducible Treg cells. Naive $CD4^+CD25^-$ T cells were isolated from spleens of c-$Jun^{WT/WT}$ and c-$Jun^{AA/AA}$ mice and stimulated ex vivo with anti-CD3 and -CD28 monoclonal Abs. To induce Treg cells ($CD4^+CD25^+Foxp3^+$) generation from primary T cells ($CD4^+CD25^-Foxp3^-$), cells were treated with TGF-β alone or TGF-β plus IL-2 or left untreated (control). Percentage of Treg cells was determined by FACS analysis. (*A*) Representative FACS analysis of Foxp3 vs. CD4. (*B*) Representative FACS analysis of Foxp3 vs. CD25.

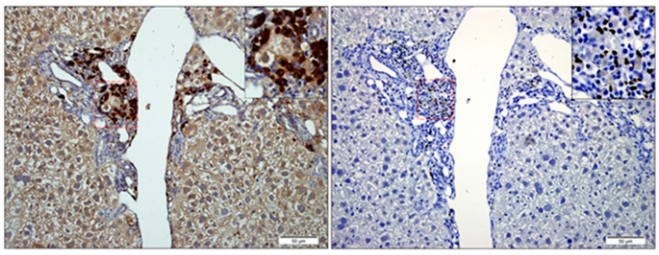

Fig. S8. Treg cells intermingle between macrophages in $Mdr2^{-/-}$ mouse livers. Representative immunohistochemical stains for CCL17 and Foxp3 on serial liver sections of 11-mo-old $Mdr2^{-/-}$ mice are shown. *Inset* shows higher magnification of the boxed region. (Scale bars: 50 μm.)

Table S1. Primers used for qPCR analysis

Target gene	Forward primer	Reverse primer
Foxp3	agccatggcaatagttccttccca	tcggataagggtggcataggtgaa
TGFβ1	accaactattgcttcagcttcagctccac	gatccacttccaacccaggtc
IL-10	ggttgccaagccttatcgga	acctgctccactgccttgct
CCL17	agtgctgcctggattacttcaaag	ctggacagtcagaaacacgatgg
CCL2	aagccagctctctcttcctcca	gcgttaactgcatctggctga
CCL22	taacatcatggctaccctgcg	tgtcttccacattggcacca
iNOS	gccaccaacaatggcaaca	cgtaccggatgagctgtgaatt
IFN-γ	tccgagcagagatcttcaggaa	tgcaaccaccactcattctgag
IL-12p40	ggaagcacggcagcagaata	aacttgagggagaagtaggaatgg
CXCL10	ccgtcattttctgcctcatcc	ccctatggccctcattctca
TNF	gaaaagcaagcagccaacca	cggatcatgctttctgtgctc
Actin	cccaaggccaaccgcgagaagat	gtcccggccagccaggtccag
PP1A	tgtaaagtcaccaccctggcacat	cgcgtctccttcgagctgtttg
HPRT	ggtaagcagtacagccccaaa	agggcatatccaacaacaaactt
Myc	tgagcccctagtgctgcat	agcccgactccgacctctt

Table S2. Primers used for genotyping

Genotype	Forward primer	Reverse primer
$Mdr2^{-/-}$	gctgagatggatcttgag	gtcgagtagccagatgatgg
Neo	tgtcaagaccgacctgtccg	tattcggcaagcaggcatcg
Jun^{AA} & Jun^{FF}	ctcataccagttcgcacaggcacaggcggc	ccgctagcactcacgttggtaggc
AFP–Cre	cggtcgatgcaacgagtgatgagg	ccagagacggaaatccatcgctcg